Hydrophobic silver nanoparticles interacting with phospholipids and stratum corneum mimic membranes in Langmuir monolayers.

Martín E. Villanueva[a], *Anabel E. Lanterna*[b] *and Raquel V. Vico**[a]

[a]Instituto de Investigaciones en Fisicoquímica de Córdoba (INFIQC-UNC-CONICET), Departamento de Química Orgánica. Facultad de Ciencias Químicas, Universidad Nacional de Córdoba. Haya de la Torre y Medina Allende, Ciudad Universitaria, X5000HUA, Córdoba, Argentina.

[b] Department of Chemistry and Biomolecular Sciences and Centre for Advanced Materials Research, University of Ottawa, Ottawa, Ontario, Canada K1N 6N5.

AUTHOR EMAIL ADDRESS AND TELEPHONE NUMBER

rvico@fcq.unc.edu.ar

TE: +54-0351-5353867 ext. 53318

AUTHORS' ORCID NUMBER

Martín E. Villanueva: 0000-0002-5289-3774

Anabel E. Lanterna: 0000-0002-6743-0940

Raquel V. Vico: 0000-0002-1982-8823

ABSTRACT

The interaction of hydrophobic silver nanoparticles with different phospholipids and stratum corneum mimic (SCM) membranes is studied in Langmuir monolayers. Thus, silver nanoparticles coated with oleic acid (AgNP-OA) were synthesized, characterized and incorporated in Langmuir monolayers of single phospholipids –having different chain length, saturation degree and phase state– or of a SCM mixture. The incorporation of AgNP-OA to the lipid monolayers generated an expansion of the monolayers and a decrease of the surface compressional modulus compared to the pure lipid. X-ray photoelectron spectroscopy (XPS) suggested that the zwitterionic choline-phospholipids can be adsorbed onto the nanoparticles' surface, which is relevant considering that phospholipids are the major constituents of the cell membrane. We also studied the changes in the topography at the mesoscale level using Brewster angle microscopy. We found the most prominent changes in the lipids with liquid-condensed phase, such as SCM, showing segregation of their components. This could have major implications in the barrier function of the membrane, affecting for example the skin permeability towards hydrophobic nanoparticles. Finally, the capability of hydrophobic AgNP-OA for delivering Ag^+ ions was studied in aqueous media in the absence and presence of phospholipids. In both conditions, AgNP-OA released Ag^+ at reported-bactericidal concentrations, being double in the presence of phospholipids.

KEYWORDS

Silver nanoparticles, nano-biointerface, phospholipids, stratum corneum, Langmuir monolayers, silver ion delivery, phosphatydilcholine adsorption.

INTRODUCTION

Silver-based compounds and silver nanoparticles (AgNP) have been used for years as antibacterial and antifungal agents, and are largely employed in surgical, hygienic and burn supplies due to their antimicrobial properties.[1] Silver NPs with diameters smaller than 100 nm, however, have shown higher antimicrobial activity when compared with other silver non-nanoparticulate compounds.[1–3] This can be attributed to the large surface-to-volume ratio of NP that provides better contact with the media and favor the continuous release of silver ions (Ag^+), considered one of the biologically active species of silver.[1,4,5] It is well known that ionization of metallic silver is related to the surface area exposed, and it has been proved that the rate of Ag^+ release is hundred-times higher from silver nanocrystals than from silver bulk materials.[1] Additionally, some reports suggest that AgNP can have antibacterial properties non-related to the release of silver ions; thus, the NP entities can affect the normal cell machinery due to changes in proteins, genetic material, and cellular membranes.[5–7] Liu *et al* have made relevant physicochemical studies regarding the fate of Ag^+ and AgNP present in biological media. They have demonstrated that AgNP experience a wide range of biochemical transformations, including oxidative dissolution in gastric acid, thiol and selenium binding and exchange, as well as the generation of secondary zero-valent AgNP.[4] Also, it has been demonstrated that Ag^+ species induce ROS generation in bacteria by interacting with the cell membranes.[5]

Many AgNP proposed as antimicrobial agents are stabilized with hydrophilic passive agents, usually citrate[5] or polymers[8,9]. Although they have good antimicrobial activity and compatibility with aqueous media, some difficulties may be present when they are used in lipophilic environments, especially in terms of their ability to reach and remain at the desired location.[3,10,11] For antimicrobial topical applications, hydrophobic AgNP may find several advantages over the hydrophilic ones because the hydrophobic nature of the skin, where the first barriers that AgNP need to survey are the stratum corneum and the cell membranes. Consequently, there have been considerable efforts to understand how the NP skin penetration mechanism, including their fate in the cells, as well as their mechanism of action

and toxicity, can be related to the physicochemical properties of the NP.[3,11–13] Nevertheless, NP local distribution, partition, organization at the mesoscale level, and their interactions and effect on biomembranes are yet not well-understood.[8,10,14–18] Therefore, the study of the physical interactions between AgNP and lipid membranes can contribute to the knowledge of their mechanism of action as well as their toxicity. Working with model biomembranes offer many advantages compared to working with living cells since the composition and organization can be easily controlled and the changes produced upon interaction can be directly measured.[8,14,19–21] Among the various biomembranes models, such as supported lipid bilayers[22] and liposomes[23], Langmuir films are excellent to study the membrane biophysics considering that a biological membrane can be conceived as two weakly coupled monolayers.[24–27] Langmuir monolayers studies provide valuable knowledge to understand for example how the interaction of amphiphilic drugs or transmembrane proteins occurs in cells. Also, the reproducibility of results and the correspondence with *in vitro* and *in vivo* pharmacological or toxicological behavior further support their use.[24,28] Other advantageous biomembranes models can be simulated by computational modeling.[29] For instance, Gupta and Rai used molecular dynamics simulations to study the effect of the surface charge and size of gold nanoparticles (AuNP) on skin permeability.[10] They simulated a skin lipid biomembrane composed by a ceramide, a long chain fatty acid, and cholesterol and demonstrated that neutral hydrophobic AuNP can disrupt the bilayer of the skin model, enter, and remain on it; whereas, the positive- or negative-charged AuNP can only be adsorbed at the interface of the skin model bilayer. Moreover, they found that the permeability of the hydrophobic AuNP is several times higher when compared with their hydrophilic counterparts.[10]

Considering the importance of the interaction of NP with biomembranes, and the role of the released silver ions for antimicrobial applications, the use of hydrophobic AgNP that can be retained at the biomembrane could increase the local action, probably reducing the dose, and optimizing their transdermal performance. Here we synthesized hydrophobic AgNP stabilized with a natural fatty acid, oleic acid (AgNP-OA), and studied their interactions with several biomembrane models using Langmuir

films. This study aimed to elucidate how hydrophobic AgNP-OA interact with model biomembranes and to which extent the biomembrane properties can change due to the presence of this nanomaterial. Thus, we evaluated the rheological properties and topography of AgNP-OA and AgNP-OA/lipids films. For this purpose, we selected single phospholipid monolayers (main constituents of cell membranes) with different phase state, and a mixture of lipids that mimic the stratum corneum.[30] Additionally, we studied the adsorption of phospholipids onto the AgNP-OA surface using X-ray photoelectron spectroscopy (XPS). Considering the relevance of released Ag^+ for the antimicrobial activity of AgNP, we tested the capability of the hydrophobic AgNP-OA to deliver silver ions into aqueous media when they are embed into lipids. We found that AgNP-OA could deliver Ag^+ in amounts that surpass the antimicrobial concentrations reported.[5,31]

MATERIALS AND METHODS

1. Materials

Silver trifluoroacetate, isoamyl ether, cholesterol (Cho), cholesterol 3-sulfate (ChoS), lignoceric acid (LA) and 3,3′,5,5′-Tetramethylbenzidine (TMB) were purchased from Sigma-Aldrich and Oleic acid (OA) from Tetrahedron. The lipids 1-palmitoyl-2-oleoyl-*sn*-glycero-3-phosphocholine (POPC), 1,2-dimyristoyl-*sn*-glycero-3-phosphocholine (DMPC), 1,2-distearoyl-*sn*-glycero-3-phosphocholine (DSPC) and (d18:1/24:0) *N*-lignoceroyl-D-erythro-sphingosine (Cer24) were purchased from Avanti Polar Lipids (Alabaster, AL, USA). All solvents and chemicals used were of the highest commercial purity available. A Milli Q system (Millipore) was used to obtain deionized water with a resistivity of 18.2 MΩ.cm.

2. Synthesis of silver nanoparticles coated by oleic acid (AgNP-OA)

Silver nanoparticles were synthesized by thermal reduction of silver trifluoroacetate in isoamyl ether in the presence of oleic acid (OA) at 160 ºC under nitrogen atmosphere according to the procedure reported

by Ling *et al*.[32,33] The purification of AgNP-OA was performed by precipitation of the nanoparticles using ethanol, followed by 10 min of sonication and 10 min of centrifugation at 3000 rpm in order to remove the excess of oleic acid. Five cycles of ethanol washing, sonication, and centrifugation were performed and finally the AgNP-OA were dried under N_2. FT-IR spectroscopy confirm the presence of a monolayer of OA covering the silver *core* in accordance with literature, see **Figure S1**.[34–36]

A stock suspension of AgNP-OA was prepared in distilled *n*-hexane and stored at -20 ºC. The typical concentration of the AgNP-OA stock suspension was 1 mg/mL (or 1.9 μM). The molar concentration was calculated by considering that the average nanoparticle molar mass that was estimated as 529 KDa. The molar mass of AgNP-OA was assessed based on their chemical characterization. For this, we assumed that the particles are covered by an OA monolayer and we used the AgNP average diameter determined by TEM and the specific density of silver. (see **Equation S1**).[21,37] Additionally, the total amount of silver in the *n*-hexane stock dispersion was quantified by using a colorimetric method based in the sensing probe 3,3′,5,5′-tetramethylbenzidine (TMB) as described below.[38]

3. Characterization of AgNP-OA

3.1 Fourier transform-infrared spectroscopy (FT-IR)

FT-IR spectra were obtained using a Thermo Scientific Nicolet iN10 Infrared Microscope operating between 500 and 4000 cm^{-1} with a resolution of 4 cm^{-1}. AgNP-OA sample was deposited and dried onto a AgBr disk. FT-IR spectra confirmed that AgNP-OA were under protection of a single layer of OA[34,36], where the carboxylate group was interacting with the silver surface and the hydrocarbon chains were pointing towards the exterior, leading to the NP hydrophobic properties. FT-IR spectra of AgNP-OA and OA are shown in **Figure S1**.

3.2 UV-Visible spectroscopy

UV–Vis spectra of AgNP-OA dispersed in *n*-hexane were measured on an HP Multispect 1501 spectrophotometer. The surface plasmon resonance (SPR) band showed a maximum absorbance at 413 nm. The stability of AgNP-OA was monitored by UV-Vis during 30 days since the preparation date (**Figure S2)**.

The biotechnological applications of nanomaterials require to keep their physicochemical properties constant for a reasonable period of time, therefore we evaluated the stability of the stock dispersion of hydrophobic AgNP-OA. The SPR maximum position and the intensity did not change for at least 15 days; beyond that the absorbance droped about 10% probably due to nanoparticle precipitation. Nevertheless, the initial absorbance is recovered after sonication (15 min) of the stock dispersion. No shift in the SPR was observed indicating the absence of aggregates or the coalescence of the NP as shown in **Figure S2**.

3.3 Transmission electron microscopy (TEM)

TEM images were acquired with a Siemens Elmiskop 101 microscope operated at an accelerating voltage of 80 kV. The average size of the silver *core* was determined as 5.2 ± 0.6 nm using the Image J software, **Figure S3**. Statistical analysis was obtained by measuring the diameter of ~3000 nanoparticles. TEM images show that AgNP-OA maintained the same morphology and mean average size after being stored in an *n*-hexane stock dispersion for at least 50 days, **Figure S3**.

3.4 X-Ray powder diffraction

X-Ray diffraction pattern was collected overnight with a Philips PAN analytical X'pert using Cu Kα radiation beam (λ=0.15406 nm) operated at a voltage of 40 kV and current of 30 mA in the range 20–80^0 (2θ). The X-Ray diffraction pattern shows the typical signal expected for pure silver metal (Ag(0)) with face-centered cubic symmetry[39], **Figure S4**.

4 Langmuir monolayers

The Langmuir film of pure AgNP-OA, pure lipids (or lipids mixtures) and AgNP-OA/lipids were obtained by seeding a stock solution of the corresponding sample at the air-water interface of a Langmuir trough. POPC, DMPC, and DSPC solutions were prepared in chloroform. The stratum corneum mimic (SCM) mixture was prepared by mixing Cer24, LA, Cho in a proportion 1:1:1 with the addition of ChoS in 5 wt % using *n*-hexane:ethanol (0.98:0.02) as solvent.[30,40,41]

The samples containing AgNP-OA/lipids were typically prepared by mixing adequate volumes of the lipid stock solution and the AgNP-OA stock dispersion in *n*-hexane to obtain a mole fraction of AgNP-OA ($X^{AgNP-OA}$) equal to 0.0005 (corresponding to 0.5 mg of AgNP-OA per mL or 0.95 μM AgNP-OA). The total amount of silver in each AgNP-OA/lipids stock sample was verified by the TMB colorimetric method (*vide infra*).[38]

The monolayers were obtained by spreading the pure AgNP-OA, pure lipid (or lipids mixture) or AgNP-OA/lipids solution at the aqueous interface of a KSV minithrough equipment (KSV, Helsinki, Finland) using Milli Q water as subphase, and waiting 10 minutes to allow for solvent evaporation before compression. The films were compressed at a rate of 10 mm/min at (23 ± 1) ºC. The absence of surface active impurities in the subphase and spreading solvent was daily checked.[21] Surface pressure (π) was measured by a platinized sensing plate. At least three surface pressure versus mean area isotherms were measured and averaged.

To evaluate deviations from the ideal behavior, the average experimental isotherms of the mixed AgNP-OA/lipids monolayers were compared to the ideally mixed films. The ideal isotherms of mixed films were calculated according to Equation (1):

$$A_{ideal}=[A^{AgNP-OA} \cdot X^{AgNP-OA} + A^{L} \cdot X^{L}]_{\pi} \qquad (1)$$

where A_{ideal} is the calculated area at constant surface pressure (π) for ideal mixed films (this is, films with an ideal mixing behaviour –no interactions–), while $A^{AgNP-OA}$, A^{L} are the areas corresponding to the pure

AgNP-OA and pure lipid, and $X^{AgNP\text{-}OA}$, X^{L} are the mole fractions of the AgNP-OA and pure lipid, respectively.

The interfacial elastic modulus of area compressibility, which reflects variations of the film in–plane elasticity, was calculated as $C_s^{-1} = -A(d\pi/dA)$, where C_s is the compressibility and π is the surface pressure measured at each area (A) point of the isotherm. The in-plane elasticity of AgNP-OA mixed with the different lipids was obtained from the experimental Langmuir isotherm measurements and compared to the elasticity of ideal mixed films. The latter was calculated for the binary mixtures using the C_s^{-1} of the pure components, the mole fractions ($X^{\mathrm{AgNP-OA}}$ and X^{L}), and the mean molecular area ($A^{\mathrm{AgNP-OA}}$ and A^{L}) in the mixture at the corresponding π as shown in Equation (2):[42,43]

$$\overline{C_s^{-1}} = \left(X^{\mathrm{AgNP-OA}} \left(\frac{C_s^{-1} A g_{\mathrm{AgNP-OA}}}{A_{\mathrm{AgNP-OA}}} \right)_{\pi} + X^{L} \left(\frac{C_s^{-1}}{A_L} \right)_{\pi} \right) \left(X^{\mathrm{AgNP-OA}} A^{\mathrm{AgNP-OA}} + X^{\mathrm{L}} A^{\mathrm{L}} \right)_{\pi} \qquad (2)$$

5 Surface topography and morphology characterization

The surface topography, morphology and texture of the films were studied by Brewster Angle Microscopy (BAM). The images were obtained with an auto-nulling EP^3–BAM (Nanofilm Technologie GmbH, Göttingen, Germany) using a 20x objective and captured with a cooled charge-coupled device (CCD) camera with a speed of 25 Hz. The wavelength of the laser beam was 532 nm and the angle of incidence was set at 53.1°. The surface pressure was measured with a KSV minithrough mounted under the microscope. In BAM, the intensity of the reflected light represents an operational "optical thickness" that is proportional to the thickness (*d*) and refractive index (*n*) of the film.

6 XPS analysis of phospholipid adsorption on AgNP-OA

The surface chemical compositions were analyzed by X-ray photoelectron spectroscopy (XPS) and the spectra were collected using a Kratos analytical model Axis Ultra DLD, using monochromatic aluminum Ka X-rays at 140 W. XPS data were analyzed using CasaXPS software, Version 2.3.15 and all

fittings obtained using a Gaussian 30% Laurentian and a Shirley baseline. The peak positions were internally referenced to the C 1s peak at 284.8 eV.

HR XPS were performed to evaluate if phospholipids adsorbed onto the silver nanoparticle surface. Samples were prepared as follows: 200 μL of AgNP-OA/POPC stock dispersion ($X^{AgNP-OA}$= 0.0005) were placed in a vial and dried until solvent complete evaporation; after that 2 mL of Milli Q water was added and the samples were vigorously stirred at room temperature during 4 days. In order to remove the free POPC from the dispersion the sample was centrifuged at 3000 rpm for 10 min, the supernatant discarded and the pellet suspended in 2 mL of chloroform. Subsequently, two more centrifugation/washing cycles with chloroform were performed. Finally, the pellet was resuspended in 50 μL of chloroform and deposited on a previously cleaned (H_2SO_4/HNO_3 2:1 mixture) silicon wafer. Additionally, 50 μL of the last supernatant were also seeded on a silicon wafer in order to confirm there was no POPC residue in the solution. XPS spectra obtained for OA, POPC and AgNP-OA are shown in **Figure S5-S7**.

7 Quantification of silver

Silver ions were quantified following the methodology reported by González-Fuenzalida *et al*[38] based on the use of the colorimetric sensing probe TMB that allows measuring Ag^+ in the presence of AgNP. Typically, a calibration curve was constructed by adding 1.2 mL of an aqueous $AgNO_3$ solution (concentration ranging between 2 to 10 ppm) to 100 μL of an ethanolic TMB solution (10 mM) previously mixed with 200 μL of NaAc/AcH (pH= 4, 1M) buffer solution. After the optimum reaction time (15 min), the absorbance at 655 nm was measured. A typical calibration curve is shown in **Figure S11**. Silver quantification was performed by triplicate at 25 ºC.

In order to determine if hydrophobic AgNP-OA were able to release Ag^+ in aqueous media, the amount of silver ions, in the presence of AgNPs, was quantified. For this 200 μL of AgNP-OA stock dispersion (containing ~0.82 mg Ag per 1 mg/mL AgNP-OA) or 200 μL of AgNP-OA:POPC or AgNP-OA:DMPC with a $X^{AgNP-OA}$= 0.0005 (containing ~0.41 mg Ag per 0.5 mg/mL AgNP-OA), were placed in a glass vial

and the organic solvent evaporated; then 2 mL of Milli Q water (or 2 mL of 145 mM NaCl aqueous solution) were added, and the samples vigorously stirred to avoid precipitation. Aliquots of 217 μL of each sample were taken at different times. Each aliquot was treated by adding 100 μL of TMB solution (10 mM in ethanol) and 683 μL of NaAc/AcH (pH= 4) buffer solution. The measurements were run in water or in the presence of NaCl in order to compare if the presence of chloride ions can affect the release of silver ions.

To quantify the total silver present in the AgNP-OA stock dispersion in *n*-hexane, AgNP-OA were previously digested with HNO_3 to completely oxidize Ag(0) into Ag(I). For this 1 mg of AgNP-OA were mixed with 160 μL of HNO_3 65%, once the solid was dissolved, 200 μL of NaOH 50% P/V were incorporated in order to neutralize the proton excess and the mixture was raised up to 2 mL with water. An aliquot of 50 μL of the above solution was placed in a glass vial and leveled to 1.2 mL with buffer. Then, the buffer/TMB solution (NaAc/AcH, 200 μL, 1 M, pH= 4; TMB 100 μL, 10 mM in ethanol) was added to the sample and the absorbance at 655 nm was monitored after 15 minutes of reaction.

RESULTS AND DISCUSSION

AgNP-OA stability, organization and mechanical properties at the air-water interface

The organization of AgNP-OA at the air-water interface was studied by means of Langmuir isotherms (π vs. mean area). **Figure 1** shows the compression isotherms and the surface compressional modulus (C_s^{-1}) obtained for AgNP-OA. The film formed by these hydrophobic silver nanoparticles is highly stable upon compression and allow evaluating the entire isotherm up to the collapse (π_c) of the film, where 2D to 3D transitions occurs and volume material or multilayers are formed. Noteworthily, isotherms of Langmuir films containing hydrophilic nanoparticles in general cannot be entirely investigated because the desorption of NP occurs from the interface to the subphase before reaching the collapse of the film.[8,14,19] Interestingly, here we show that these hydrophobic AgNP-OA exhibited a high collapse surface pressure at about 50 mN/m. Furthermore, once the AgNP-OA film is compressed up to near the collapse, upon expansion, the isotherms practically do not present hysteresis indicating that the system does not retains energy, for example in the form of new particle-particle interactions (**Figure S8**). This suggests that no clustering or agglomerations are formed between the NP, even when they are forced to be in intimate contact. These results are in contrast to what was found for hydrophobic magnetite nanoparticles of similar size and same stabilizer (OA), where the NP films show an important hysteresis.[21] Consequently, the inter–particle interactions established at the air-water interface are not only dictated by the molecules that stabilize the nanoparticles and directly exposed to the media, but also the nature of the NP *core* (*i.e.*, silver versus magnetite) plays an important role on the regulation of the inter–particle interactions and the organization at the interfaces.

Using the surface compressional modulus (C_s^{-1}) one can get insights on the physical state of a film and determine the in-plane surface elasticity or fluidity.[18,44] For instance, for classical amphiphiles such as lipids, the C_s^{-1} allows to know the phase state and infer the packing order in a monolayer.[45] Since NP are not classic amphiphiles, it is not appropriate to directly compare the C_s^{-1} values from NP films to

that obtained for typical surfactants. However, in the case of films formed by NP, the C_s^{-1} is useful to detect changes in the organization of the NP at interfaces. By inspection of C_s^{-1} of the AgNP-OA film (**Figure 1A**), we can observe that upon compression from the lit-off pressure up to about 12 mN/m (*i.e.*, from 20000 to 7000 Å^2/particle), the C_s^{-1} values varies from 5 to 20 mN/m. The behaviour of the C_s^{-1} values in this region indicate that the particle surface density is fluctuating without significant changes in the in-plane elasticity and organization. This behaviour is also noticeable in the surface topography obtained using BAM imaging, where we can see conglomerates of NP separated by void space at the air-water interface, **Figure 1B**. Beyond 12 mN/m the surface pressure, the surface compressibility modulus, as well as the optical thickness of the film sharply increase. The void space is filled because the NP merged and this has as consequence the steep increment in the surface pressure and surface compressional modulus that reveal a less flexible film. A similar behavior was reported by You *et al* for Langmuir monolayers composed by AgNP capped with oleilamine.[46] The limiting extrapolated area to zero surface pressure (A_0) for AgNP-OA, which corresponds to the cross section of the NP in the more condensed region of the isotherm, is ~ 6300 Å^2/particle. This value is similar to that calculated by the theoretical sectional area of AgNP-OA (~ 5600 Å^2/particle) taking into account the diameter of the silver *core* (5.2 nm) and the length of two fully extended oleic acid chains (1.75 nm each OA),[47] as shown in the inset in **Figure 1A**. All these findings suggest that beyond ~12 mN/m the AgNPs-OA are organized in a 2D array up to near the collapse of the film.

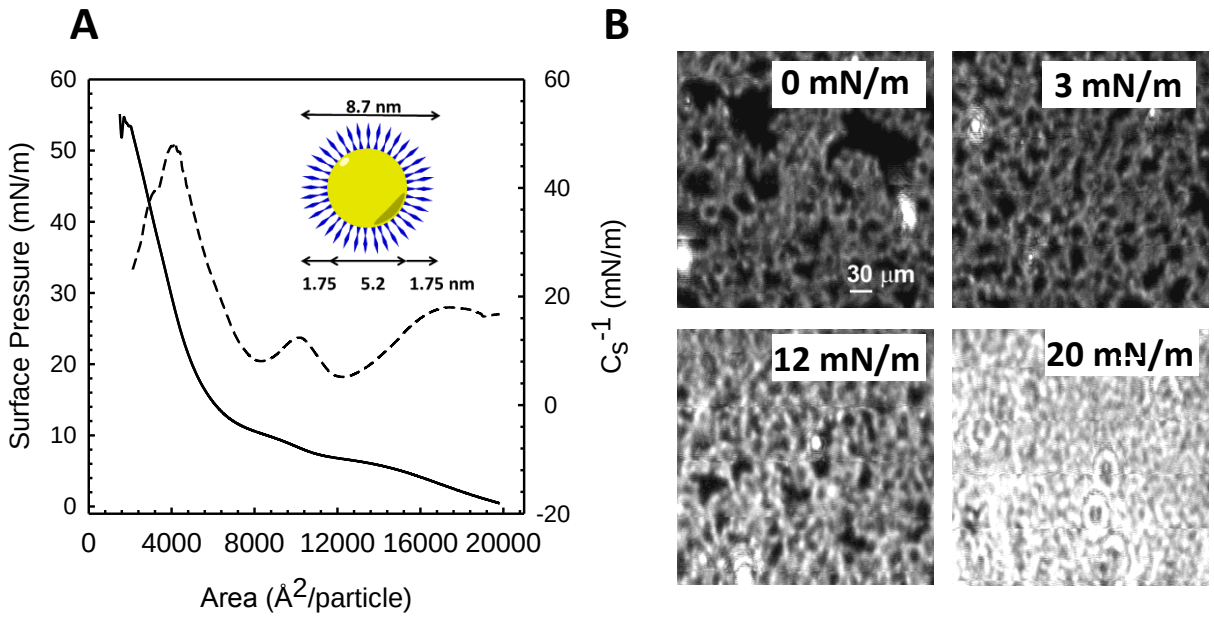

Figure 1. A) Variation of surface pressure (solid line) and surface compressional modulus (C_s^{-1}, dashed line) with the average area of AgNP-OA at the air-water interface. The inset shows the size of AgNP-OA (yellow Ag *core*, blue OA). The theoretical sectional area calculated (Ag *core* + 2 oleic acid molecules) was ~ 5600 Å^2. B) BAM images of the AgNP-OA topography at the air-water interface upon the indicated surface lateral pressure. Scale bar 30 μm.

Interaction of AgNP-OA with model biomembranes.

In order to explore how the hydrophobic AgNP-OA interact with model biomembranes and to which extent the properties of both are modified, we studied different biomembranes models (*i.e.*, different composition and phase state). The lipid monolayers evaluated include pure DMPC, POPC, or DSPC, and a lipid mixture that mimic the composition of the stratum corneum (SCM).[30] The phospholipids selected for this study contain acyl chains of various length and saturation degree, and therefore adopt different phase states at the air-water interface. Thus, DMPC (saturated PC) and POPC (unsaturated PC) adopt a liquid-expanded (LE) phase over the entire compression isotherm, whereas

DSPC (saturated PC) exist in a liquid-condensed phase (LC). On the other hand, SCM, constituted by Cer24/LA/Cho 1:1:1 and 5% w/w ChoS,[30,48] is a quaternary monolayer that was previously studied by compression isotherms and diffusion properties showing LC behavior.[30]

Upon analysis of the surface pressure-area isotherms (**Figure 2**) at the air-water interface, we were able to see how the presence of the hydrophobic AgNP-OA induced a shift of the lipid isotherms towards higher areas compared to the isotherms expected for the ideal NP-lipid mixture. This indicates that AgNP-OA are incorporated into the film as a non-ideal mixture. Comparing the different lipids, the highest displacement in areas accounts for SCM followed by the saturated phospholipids DSPC and DMPC, and finally the unsaturated POPC. Additionally, we evaluated the C_s^{-1} values for AgNP-OA/lipids mixtures as a function of the surface pressure (see **Figure S9**). The C_s^{-1} value provides essential information about membrane properties such as fluidity; thus, it provides a quantitative measurement of the monolayer in-plane packing elasticity. When C_s^{-1} for AgNP-OA/lipids mixtures is evaluated as a function of the surface pressure and compared with that of the pure lipids (see **Figure S9**), the general trend observed is a decrease in the C_s^{-1}. LC phase lipids, particularly SCM, are more susceptible to the presence of the particles than LE phase lipids. The films composed by AgNP-OA/DSPC or AgNP-OA/SCM (LC phase lipids) showed a marked decrease in C_s^{-1} at low and high surface pressure indicating that the films become more compressible and acquired a more expanded or fluid character (lower C_s^{-1} values) in reference to the pure lipid. We can assume that LC phase lipids experience a greater disorder at the molecular level of organization introduced by the AgNP-OA. In the case of SCM, the decrease of the C_s^{-1} values caused in the presence of AgNP-OA may have important implications as it can modify the cross-membrane processes, the skin permeability, and the barrier function of the stratum corneum.

Furthermore, we were able to map the topography of the films at different surface pressures using BAM. When DMPC, POPC, DSPC and SCM films were observed by BAM they showed homogenous topography along the entire isotherm since the gaseous phase is left.[21,30] The BAM images of the different AgNP-OA/lipid mixtures acquired at different surface pressures clearly show the presence of AgNP-OA

as brilliant spots at the interface that remained even after compression without any particular pattern. Besides, SCM in the presence of AgNP-OA presented the coexistence of different phases up to ~8 mN/m (**Figures 2 and S10**), suggesting the segregation or demixing of their constituents. This topographic pattern is consistent with the large area displacement observed for AgNP-OA/SCM isotherm as well as with the significant change in C_s^{-1} values compared to those obtained using SCM only. It is possible that the greater changes evidenced for SCM in the presence of AgNP-OA are due to the presence of the cholesterol in the membrane, as it has previously been demonstrated by Gupta and Rai[10] studying the effect of anionic, cationic and hydrophobic gold nanoparticles on the skin permeability.

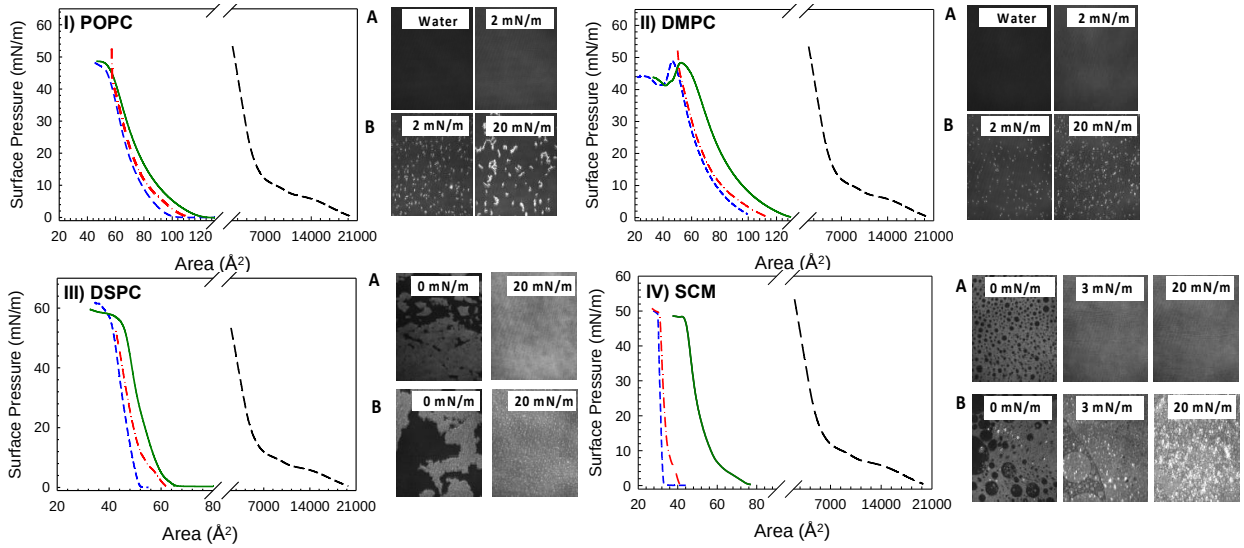

Figure 2. Surface pressure-Area isotherms at the air-water interface for I) POPC, II) DMPC, III) DSPC and IV) SCM in the absence or in the presence of AgNP-OA. Pure lipid/s (blue, short-dashed line), pure AgNP-OA (black, long-dashed line), experimental (green, solid line) and ideal mixed monolayer with $X^{AgNP\text{-}OA}$=0.0005 (red, dot-dashed line). BAM images showing the topography of the films in the absence (panels A) or in the presence (panels B) of AgNP-OA at the indicated surface pressure. Images are 250 × 200 μm.

Adsorption of phospholipids at the AgNP-OA surface

When we study the interaction of NP with biomolecules it is important to describe their interface; *i.e.,* the biomolecules can be present on the NP surface either by interaction with the NP surface ligands

(*i.e.* van der Wall or electrostatic forces) or undergoing ligand exchange.[19,49,50] It is well known that in biological fluids NP have the ability to adsorb proteins and form a protein layer, known as protein corona,[49–51] which dictates the biological response to the NP. Understanding the interaction of nanomaterials with biological systems becomes a key feature for their fate, safe and efficient applications. Nevertheless, only few studies reported about the adsorption or ligand exchange among lipids and nanoparticles. Lipids represent the major components of cell membranes, and therefore they are directly related to the role of the membrane as a barrier towards NP permeation (or endocytosis). This issue has special concerns for those nanoparticles proposed for topical use, such as those designed as antimicrobial agents or as part of cosmetics or sunscreen. Segota et al studied the interaction of hydrophobic Ag- and Au-NPs caped with a stearyl-based ligand and DMPC using as biomembrane model supported lipid bilayers.[22] Interestingly they found that the hydrophobic part of the stearyl-derived ligand stays within the hydrophobic region of the bilayer and fuses with the surrounding hydrocarbon chain of the lipid. This leads to a reorganization of the bilayer that result in an increased amount of lipid in the region surrounding the NPs and a decrease in the region that are located between them.[22]

To further understand the interaction of the phospholipids and the silver nanoparticles, we evaluated the presence of phospholipid at the AgNP-OA surface by XPS analysis using POPC as the model lipid. **Figures S7-S9** show the XPS spectra obtained for OA, POPC and AgNP-OA, respectively, and their corresponding characterization. In order to evaluate the interaction between POPC and AgNP-OA, we mixed the nanoparticles and the lipid in aqueous media for about 96 h. After that, several centrifugation and washing cycles were performed in order to remove the free POPC and evaluate the resulting pellet. The HR XPS spectra of the AgNP-OA/POPC pellet shown in **Figures 3A-C** are compared to those obtained from the wash chloroform from the last washing cycle (**Figures 3D-F**). First we notice in the AgNP-OA/POPC pellet the presence of the Ag 3d signals (**Figures 3A)** corresponding to the presence of AgNP-OA and the N 1s and P 2p (**Figures 3B-C)** signals belonging to the POPC. On the other hand, the complete removal of POPC was confirmed by the absence of the corresponding XPS

signals (P 2p and N 1s) in the wash chloroform used in the last washing cycle (**Figures 3E-F**). Additionally, no residues of AgNP-OA are detected (absence of Ag 3d signal in **Figure 3D**). These results indicate that certain amount of phospholipid remains adsorbed on the nanoparticle surface, either by physisorption (likely favored by Van der Waals forces between POPC and the hydrocarbon chain of the oleic acid) or binding to the Ag surface through interactions with the POPC phosphate oxygen. The latter would require some empty space on the NP surface, or undergo OA-ligand exchange. Considering that phospho-choline lipids showed poor ability acting as capping agents,[52] we can expect POPC to be weakly adsorbed on the silver surface, and therefore it is unlikely to displace the OA ligands.

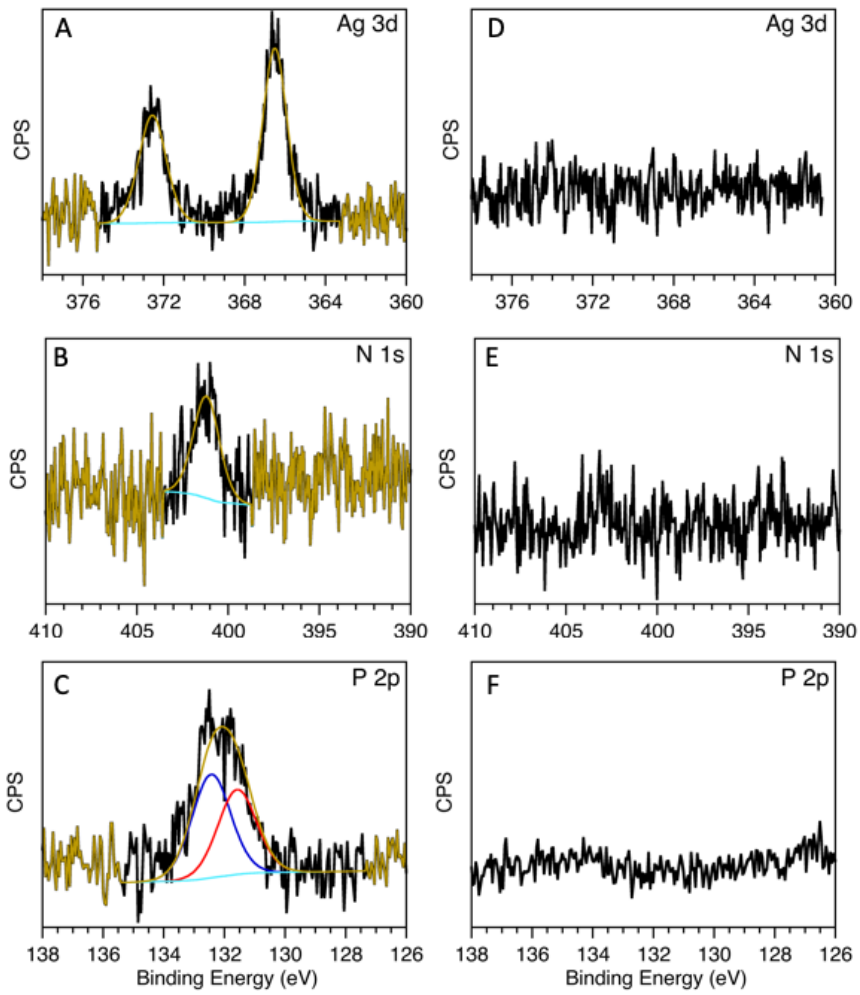

Figure 3. HR XPS spectra showing the Ag 3d, N 1s, and P 2p regions for the AgNP-OA/POPC pellet (A-C) and the wash chloroform from the last washing cycle (D-F) showing no residual POPC or AgNP-OA.

Release of silver ions from hydrophobic AgNP-OA

An important issue regarding biotechnological applications of AgNP is their ability to release Ag^+ to the surrounding media. It is well known that AgNP can progressively release Ag^+ from their crystalline *core*.[2,4] Also, the Ag^+ released from NP inside cells, activate a Trojan-horse-type mechanism that induces ROS production and lipid peroxidation that causes a lethal effect on bacteria.[5] Most of the data available,

mainly related to hydrophilic nanoparticles, reflect that the amount of Ag^+ needed for the inhibition against different microorganisms depends on the microorganism and on the nanoparticle characteristics. In general, the amount of Ag^+ required to inhibit microorganisms growth is on the nano- to micro-molar range.[5,31] Even though it has been demonstrated that hydrophilic AgNPs are successful for many biomedical applications, hydrophobic nanoparticles could possess a better compatibility with lipophilic media as they can reach, remain and disturb such environments probably reducing the dose needed. Therefore we measured the amount of Ag^+ released from the hydrophobic AgNP-OA in different media; *i.e.*, in water, in an electrolyte solution (NaCl, 145 mM), or in the presence of lipid (POPC or DMPC) suspensions in water. **Table 1** summarizes the amount of Ag^+ it was released from each sample after 5 days. The values are almost constant for at least 15 days (see **Figure S12**).

Table 1. Ag^+ released from hydrophobic AgNP-OA in different media after 5 days at 25 ^oC.

Sample	**Ag^+ ng/mL per mg AgNP-OA**
AgNP-OA (water)	4560 ± 200
AgNP-OA (NaCl 145 mM)	4480 ± 200
AgNP-OA + DMPC (water)	10047 ± 200
AgNP-OA + POPC (water)	8160 ± 200

No significant difference was found for Ag^+ released in water or in a NaCl solution, or between suspensions containing POPC or DMPC. Nevertheless, in the presence of phospholipids the amount of Ag^+ doubled that found in aqueous media. This trend can be rationalized considering that phospholipids facilitate the dispersion of the hydrophobic nanoparticles in the aqueous media, which is not possible when there is only water or an electrolyte solution. The amount of Ag^+ released after 5 days from 1 mg of AgNP-OA represents about 0.5-1.0% of the initial mass of the AgNP-OA and reaches the μM range in the conditions here explored. This result demonstrates the potential of these hydrophobic silver nanoparticles to act as antimicrobial agents compatible with lipophilic media.

CONCLUSION

In this work, we have been able to identify that hydrophobic silver nanoparticles covered with the natural fatty acid oleic acid strongly interact with model biomembranes. The presence of AgNP-OA in single phospholipid monolayers (DMPC, POPC, DSPC) or in a mixture that mimic the stratum corneum (SCM) occasioned changes in the monolayers giving higher areas than that expected for an ideal mixed film. In addition, the surface compressional modulus C_s^{-1} was lowered reflecting changes in essential membrane properties, such as fluidity. Lipids having LE or LC character were affected, but those with LC phase reflect the major changes, in especial SCM. This suggests that lipids with LC phase experienced a greater disorder at the molecular level of organization introduced by the AgNP-OA, which increase the fluidity of the films. In the case of the SCM, this can have important implications because the cross-membrane processes, the skin permeability and the barrier function of the stratum corneum could be modified in the presence of AgNP-OA. The demixing of its constituents that lead to phase segregation, as was monitored by BAM, also evidenced the effect of the AgNP-OA in the SCM films. In addition, we were able to demonstrate the adsorption of phosphocholine molecules (POPC) on the AgNP-OA surface. The complexity of the interactions among the monolayer components was analyzed at the molecular and at the mesoscale level. The presence of favorable interactions between the hydrocarbon chain of oleic acid –present in AgNP-OA– and that of the lipids, mainly through van der Waals cohesive forces, was demonstrated through XPS analysis as well as reported by Segota et al.[22] At the mesoscale level, the system adopts a supramolecular organization at the interface, far from ideal behavior, imposed most probably by steric effects.

Finally, we were able to determine that AgNP-OA can release Ag^+ in aqueous and lipophilic environments at reported bactericidal-concentration ranges. Therefore, these hydrophobic AgNP-OA can be potentially used as antimicrobial agents in lipophilic environments, such as topical applications. These results could be helpful in designing customized nanoparticles for cosmetic and transdermal applications.

ACKNOWLEDGMENT

This work was supported by SECyT-UNC, FONCYT PICT 2016-0262, Argentina and the Natural Sciences and Engineering Research Council of Canada and the Canada Foundation for Innovation. M.E.V. is a grateful recipient of a PhD scholarship awarded by CONICET. R.V.V. is a full-time researcher of CONICET.

REFERENCES

(1) Lansdown, A. B. G. A Pharmacological and Toxicological Profile of Silver as an Antimicrobial Agent in Medical Devices. *Adv. Pharmacol. Sci.* **2010**, ID 910686, 16 pages.

(2) Morones, J. R.; Elechiguerra, J. L.; Camacho, A.; Holt, K.; Kouri, J. B.; Ramírez, J. T.; Yacaman, M. J. The Bactericidal Effect of Silver Nanoparticles. *Nanotechnology* **2005**, *16*, 2346–2353.

(3) Labouta, H. I.; Schneider, M. Interaction of Inorganic Nanoparticles with the Skin Barrier: Current Status and Critical Review. *Nanomedicine NBM* **2013**, *9*, 39–54.

(4) Liu, J.; Wang, Z.; Liu, F. D.; Kane, A. B.; Hurt, R. H. Chemical Transformations of Nanosilver in Biological Environments. *ACS Nano* **2012**, *6*, 9887–9899.

(5) Long, Y. M.; Hu, L. G.; Yan, X. T.; Zhao, X. C.; Zhou, Q. F.; Cai, Y.; Jiang, G. Bin. Surface Ligand Controls Silver Ion Release of Nanosilver and Its Antibacterial Activity against Escherichia Coli. *Int. J. Nanomed.* **2017**, *12*, 3193–3206.

(6) Zhu, M.; Nie, G.; Meng, H.; Xia, T.; Nel, A.; Zhao, Y. Physicochemical Properties Determine Nanomaterial Cellular Uptake, Transport, and Fate. *Acc. Chem. Res.* **2013**, *46*, 622–631.

(7) Alarcon, E. I.; Udekwu, K.; Skog, M.; Pacioni, N. L.; Stamplecoskie, K. G.; González-Béjar, M.; Polisetti, N.; Wickham, A.; Richter-Dahlfors, A.; Griffith, M.; et al. The Biocompatibility and Antibacterial Properties of Collagen-Stabilized, Photochemically Prepared Silver Nanoparticles. *Biomaterials* **2012**, *33*, 4947–4956.

(8) Soriano, G. B.; Oliveira, S.; Camilo, F. F.; Caseli, L. Interaction of Non-Aqueous Dispersions of Silver Nanoparticles with Cellular Membrane Models. *J. Colloid Interf. Sci.* **2017**, *496*, 111–117.

(9) Yang, W.; Wu, K.; Liu, X.; Jiao, Y.; Zhou, C. Construction and Characterization of an Antibacterial/Anticoagulant Dual-Functional Surface Based on Poly L-Lactic Acid Electrospun Fibrous Mats. *Mater. Sci. Eng. C* **2018**, *92*, 726–736.

(10) Gupta, R.; Rai, B. Effect of Size and Surface Charge of Gold Nanoparticles on Their Skin Permeability: A Molecular Dynamics Study. *Sci. Rep.* **2017**, *7*, 45292.

(11) Larese, F.; Mauro, M.; Adami, G.; Bovenzi, M.; Crosera, M. Nanoparticles Skin Absorption: New Aspects for a Safety Profile Evaluation. *Regul. Toxicol. Pharmacol.* **2015**, *72*, 310–322.

(12) Larese, F. F.; D'Agostin, F.; Crosera, M.; Adami, G.; Renzi, N.; Bovenzi, M.; Maina, G. Human Skin Penetration of Silver Nanoparticles through Intact and Damaged Skin. *Toxicology* **2009**, *255*, 33–37.

(13) Smijs, T. G. M.; Bouwstra, J. a. Focus on Skin as a Possible Port of Entry for Solid Nanoparticles and the Toxicological Impact. *J. Biomed. Nanotechnol.* **2010**, *6*, 469–484.

(14) Bothun, G. D.; Ganji, N.; Khan, I. A.; Xi, A.; Bobba, C. Anionic and Cationic Silver Nanoparticle Binding Restructures Net-Anionic PC/PG Monolayers with Saturated or Unsaturated Lipids. *Langmuir* **2017**, *28*, 353–360.

(15) Guzmán, E.; Liggieri, L.; Santini, E.; Ferrari, M.; Ravera, F. Effect of Hydrophilic and Hydrophobic Nanoparticles on the Surface Pressure Response of DPPC Monolayers. *J. Phys. Chem. C* **2011**, *115*, 21715–21722.

(16) Guzmán, E.; Liggieri, L.; Santini, E.; Ferrari, M.; Ravera, F. Influence of Silica Nanoparticles on Phase Behavior and Structural Properties of DPPC-Palmitic Acid Langmuir Monolayers. *Colloids Surf., A* **2012**, *413*, 280–287.

(17) Guzmán, E.; Santini, E.; Ferrari, M.; Liggieri, L.; Ravera, F. Interfacial Properties of Mixed DPPC–Hydrophobic Fumed Silica Nanoparticle Layers. *J. Phys. Chem. C* **2015**, *119*, 21024–21034.

(18) Torrano, A. A.; Pereira, Â. S.; Oliveira, O. N.; Barros-Timmons, A. Probing the Interaction of Oppositely Charged Gold Nanoparticles with DPPG and DPPC Langmuir Monolayers as Cell Membrane Models. *Colloids Surf. B. Biointerfaces* **2013**, *108*, 120–126.

(19) Maya Girón, J. V.; Vico, R. V.; Maggio, B.; Zelaya, E.; Rubert, A.; Benítez, G.; Carro, P.; Salvarezza, R. C.; Vela, M. E. Role of the Capping Agent in the Interaction of Hydrophilic Ag Nanoparticles with DMPC as a Model Biomembrane. *Environ. Sci. Nano* **2016**, *3*, 462–472.

(20) Ábrahám, N.; Csapó, E.; Bohus, G. Interaction of Biofunctionalized Gold Nanoparticles with Model Phospholipid Membranes. *Colloid Polym. Sci.* **2014**, *292*, 2715–2725.

(21) Matshaya, T. J.; Lanterna, A. E.; Granados, A. M.; Krause, R. W. M.; Maggio, B.; Vico, R. V. Distinctive Interactions of Oleic Acid Covered Magnetic Nanoparticles with Saturated and Unsaturated Phospholipids in Langmuir Monolayers. *Langmuir* **2014**, *30*, 5888–5896.

(22) Šegota, S.; Vojta, D.; Kendziora, D.; Ahmed, I.; Fruk, L.; Baranović, G. Ligand-Dependent Nanoparticle Clustering within Lipid Membranes Induced by Surrounding Medium. *J. Phys. Chem. B* **2015**, *119*, 5208–5219.

(23) Wang, B.; Zhang, L.; Chul, S.; Granick, S. Nanoparticle-Induced Surface Reconstruction of Phospholipid Membranes. *Proc. Natl. Acad. Sci. U. S. A.* **2008**, *105*, 18171–18175.

(24) Limited, W. P. *Drug – Biomembrane Interaction Studies*; Pignatello, R., Ed.; Woodhead Publishing Limited, 2013.

(25) Brockman, H. L. Lipid Monolayers: Why Use Half a Membrane to Characterize Protein-Membrane Interactions? *Curr. Opin. Struct. Biol.* **1999**, *9*, 438–443.

(26) Brezesinski, G.; Mohwald, H. Langmuir Monolayers to Study Interactions at Model Membrane Surfaces. *Adv. Colloid Interface Sci. Colloid Interface Sci.* **2003**, *102*, 563–584.

(27) Giner-Casares, J. J.; Brezesinski, G.; Möhwald, H. Langmuir Monolayers as Unique Physical Models. *Curr. Opin. Colloid Interface Sci.* **2014**, *19*, 176–182.

(28) Peetla, C.; Rao, K. S.; Labhasetwar, V. Relevance of Biophysical Interactions of Nanoparticles with a Model Membrane in Predicting Cellular Uptake : Study with TAT Peptide-Conjugated Nanoparticles. *Mol. Pharm.* **2009**, *6*, 1311–1320.

(29) Marrink, S. J.; Corradi, V.; Souza, P. C. T.; Ingólfsson, H. I.; Tieleman, D. P.; Sansom, M. S. P. Computational Modeling of Realistic Cell Membranes. *Chem. Rev.* **2019**, DOI: 10.1021/acs.chemrev.8b00460.

(30) Zulueta Díaz, Y. D. L. M.; Mottola, M.; Vico, R. V; Wilke, N.; Fanani, M. L. The Rheological Properties of Lipid Monolayers Modulate the Incorporation of L-Ascorbic Acid Alkyl Esters. *Langmuir* **2016**, *32*, 587–595.

(31) Kim, J. S.; Kuk, E.; Yu, K. N.; Kim, J. H.; Park, S. J.; Lee, H. J.; Kim, S. H.; Park, Y. K.; Park, Y. H.; Hwang, C. Y.; et al. Antimicrobial Effects of Silver Nanoparticles. *Nanomedicine* **2007**, *3*, 95–101.

(32) Wang, Y.; Wong, J. F.; Teng, X.; Lin, X. Z. " Pulling " Nanoparticles into Water : Phase Transfer of Oleic Acid Stabilized Monodisperse Nanoparticles into Aqueous Solutions of Alpha-Cyclodextrin. *Nano Lett.* **2003**, *3*, 1155–1159.

(33) Lin, X. Z.; Teng, X.; Yang, H. Direct Synthesis of Narrowly Dispersed Silver Nanoparticles Using a Single-Source Precursor. *Langmuir* **2003**, *19*, 10081–10085.

(34) Xu, Z.; Hu, G. Simple and Green Synthesis of Monodisperse Silver Nanoparticles and Surface-Enhanced Raman Scattering Activity. *RSC Adv.* **2012**, *2*, 11404–11409.

(35) Lee, S. J.; Kim, K. Diffuse Reflectance Infrared Spectra of Stearic Acid Self-Assembled on Fine Silver Particles. *Vib. Spectrosc.* **1998**, *18*, 187–201.

(36) Mahdavi, M.; Ahmad, M. Bin; Haron, M. J.; Namvar, F.; Nadi, B.; Ab Rahman, M. Z.; Amin, J. Synthesis, Surface Modification and Characterisation of Biocompatible Magnetic Iron Oxide Nanoparticles for Biomedical Applications. *Molecules* **2013**, *18*, 7533–7548.

(37) McCarthy, S. A.; Davies, G.-L.; Gun'ko, Y. K. Preparation of Multifunctional Nanoparticles and Their Assemblies. *Nat. Protoc.* **2012**, *7*, 1677–1693.

(38) González-Fuenzalida, R. A.; Moliner-Martínez, Y.; González-Béjar, M.; Molins-Legua, C.; Verde-Andres, J.; Pérez-Prieto, J.; Campins-Falcó, P. In Situ Colorimetric Quantification of Silver Cations in the Presence of Silver Nanoparticles. *Anal. Chem.* **2013**, *85*, 10013–10016.

(39) Khanna, P. K.; Kulkarni, D.; Beri, R. K. Synthesis and Characterization of Myristic Acid Capped Silver Nanoparticles. *J. Nanopart. Res.* **2008**, *10*, 1059–1062.

(40) Pullmannová, P.; Staňková, K.; Pospíšilová, M.; Školová, B.; Zbytovská, J.; Vávrová, K. Effects of Sphingomyelin / Ceramide Ratio on the Permeability and Microstructure of Model Stratum Corneum Lipid Membranes. *Biochim. Biophys. Acta* **2014**, *1838*, 2115–2126.

(41) Mao, G.; Vanwyck, D.; Xiao, X.; MacK Correa, M. C.; Gunn, E.; Flach, C. R.; Mendelsohn, R.;

Walters, R. M. Oleic Acid Disorders Stratum Corneum Lipids in Langmuir Monolayers. *Langmuir* **2013**, *29*, 4857–4865.

(42) Ali, S.; Smaby, J. M.; Brockman, H. L.; Brown, R. E. Cholesterol's Interfacial Interactions with Galactosylceramides. *Biochemistry* **1994**, *33*, 2900–2906.

(43) Dupuy, F.; Maggio, B. The Hydrophobic Mismatch Determines the Miscibility of Ceramides in Lipid Monolayers. *Chem. Phys. Lipids* **2012**, *165*, 615–629.

(44) Brown, R. E.; Brockman, H. L. Using Monomolecular Films to Characterize Lipid Lateral Interactions. *Methods Mol Biol.* **2007**, 41–58.

(45) Davies, J. T.; Rideal, E. K. Interfacial Fenomena. **1963**.

(46) You, S. S.; Rashkov, R.; Kanjanaboos, P.; Calderon, I.; Meron, M.; Jaeger, H. M.; Lin, B. Comparison of the Mechanical Properties of Self-Assembled Langmuir Monolayers of Nanoparticles and Phospholipids. *Langmuir* **2013**, *29*, 11751–11757.

(47) Pauly, M.; Pichon, B. P.; Demortière, A.; Delahaye, J.; Leuvrey, C.; Pourroy, G.; Bégin-Colin, S. Large 2D Monolayer Assemblies of Iron Oxide Nanocrystals by the Langmuir–Blodgett Technique. *Superlattices Microstruct.* **2009**, *46*, 195–204.

(48) Gooris, G.; Bouwstra, J.; Berka, P.; Roh, J.; Palat, K.; Alexandr, H.; Vávrová, K. Ceramides in the Skin Lipid Membranes: Length Matters. *Langmuir* **2013**, *25*, 1–7.

(49) Lundqvist, M.; Augustsson, C.; Lilja, M.; Lundkvist, K.; Dahlbäck, B.; Linse, S.; Cedervall, T. The Nanoparticle Protein Corona Formed in Human Blood or Human Blood Fractions. *PLoS One* **2017**, *12*, 1–15.

(50) Kharazian, B.; Hadipour, N. L.; Ejtehadi, M. R. Understanding the Nanoparticle–protein Corona Complexes Using Computational and Experimental Methods. *Int. J. Biochem. Cell Biol.* **2016**, *75*, 162–174.

(51) Docter, D.; Westmeier, D.; Markiewicz, M.; Stolte, S.; Knauer, S. K.; Stauber, R. H. The Nanoparticle Biomolecule Corona: Lessons Learned - Challenge Accepted? *Chem. Soc. Rev.* **2015**, *44*, 6094–6121.

(52) Bakshi, M. S.; Possmayer, F.; Petersen, N. O. Role of Different Phospholipids in the Synthesis of Pearl-Necklace-Type Gold-Silver Bimetallic Nanoparticles as Bioconjugate Materials. *J. Phys. Chem. C* **2007**, *111*, 14113–14124.